Supplementary Information

Co-recycling of spent cathode and anode via redox-mediated lithiation

Zhiming Du, Peixiang Gao, Yuxiang Chen, Yingming Zhang, Yongzhi Liu, Xuejing Qiu*, Lingling Xie

School of Environmental Engineering

Henan University of Technology

Zhengzhou 450001, China

E-mail: qiuxj@haut.edu.cn.

Table of Contents

for

Supplementary Information

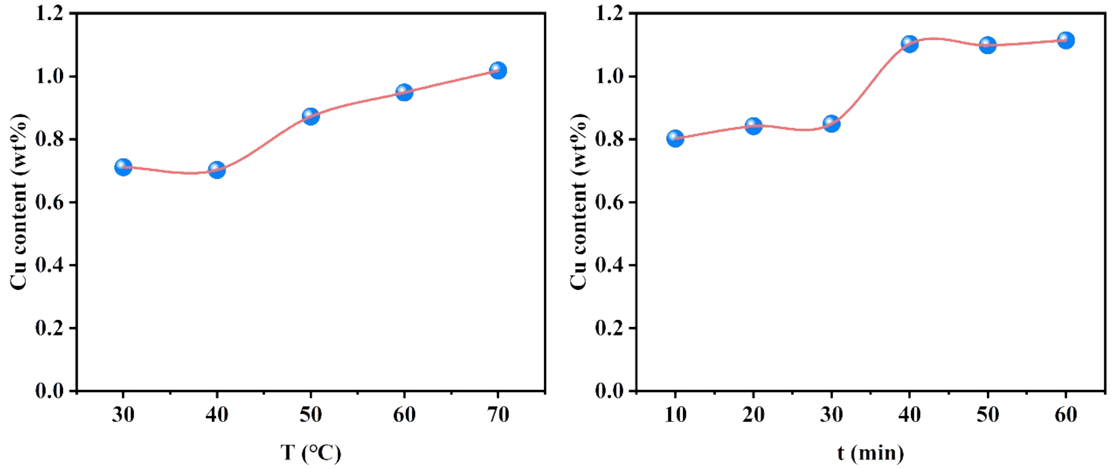

Supplementary Fig. 1 Cu content in water solution with different temperatures and times after Cu foil-graphite layer separation operation.

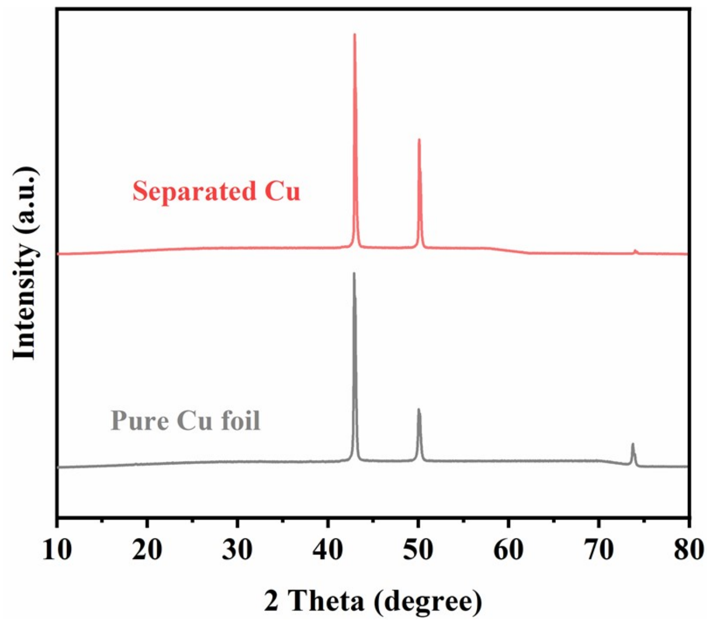

Supplementary Fig. 2 The XRD patterns of the separated and pure Cu foil.

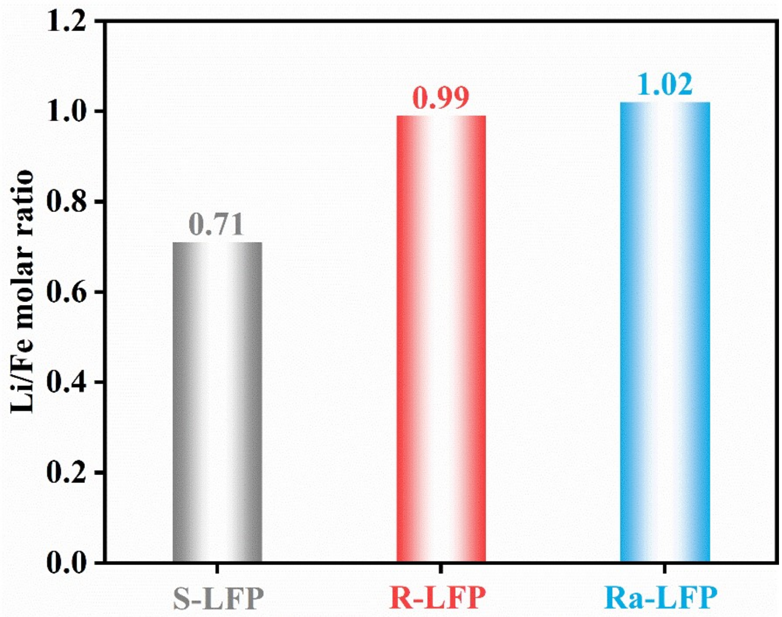

Supplementary Fig. 3 Li/Fe molar ratio of S-LFP, R-LFP and Ra-LFP based on ICP results.

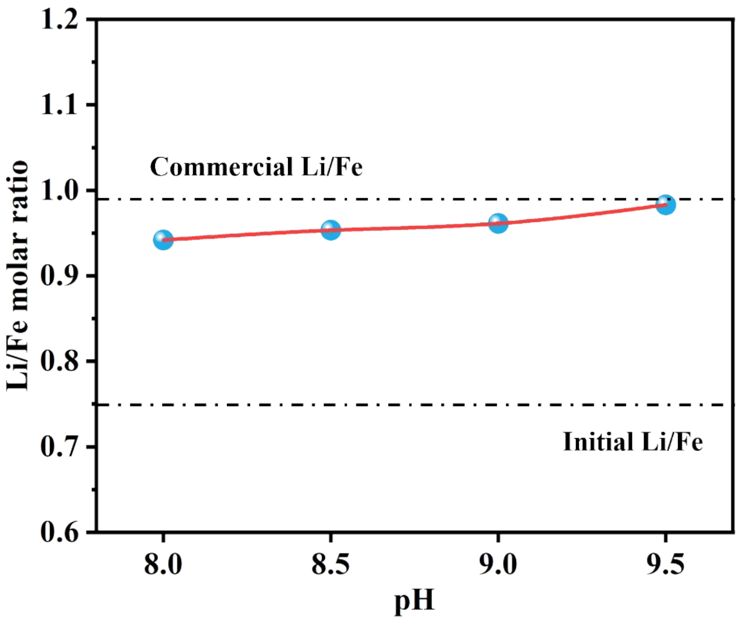

Supplementary Fig. 4 Li/Fe molar ratio of R-LFP with different pH values.

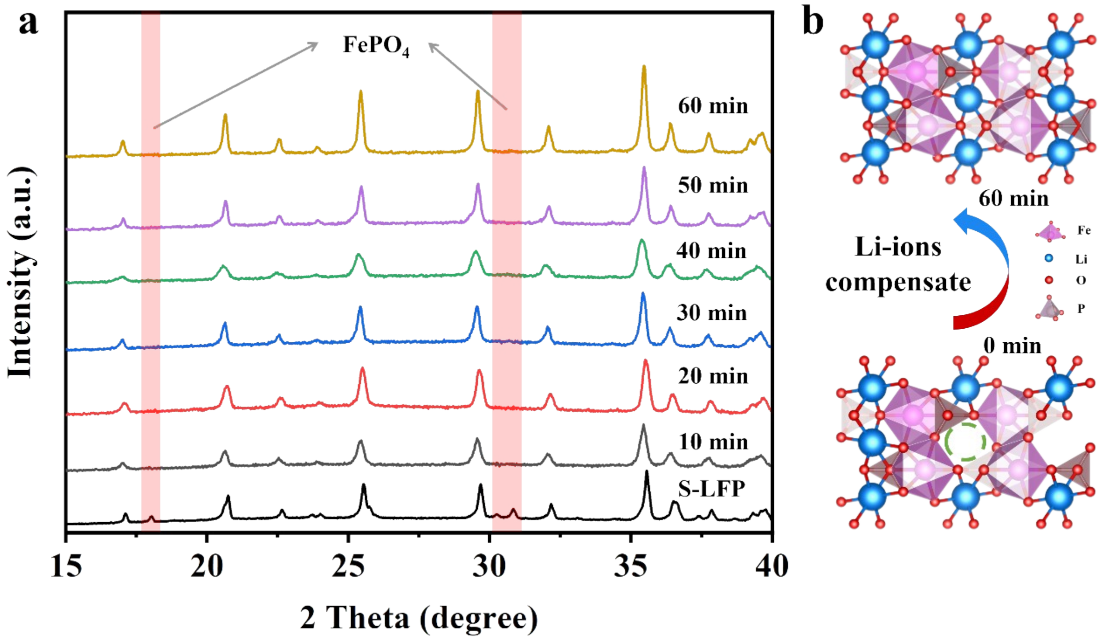

Supplementary Fig. 5 (a) XRD patterns of S-LFP and R-LFP with different lithiation time. The gradual diminishment of $FePO_4$ peaks (marked in red) shows the conversion of the $FePO_4$ phase to LFP phase. (b) Schematic showing that Li vacancies have been filled and crystalline structure recovers to the original state after direct regeneration.

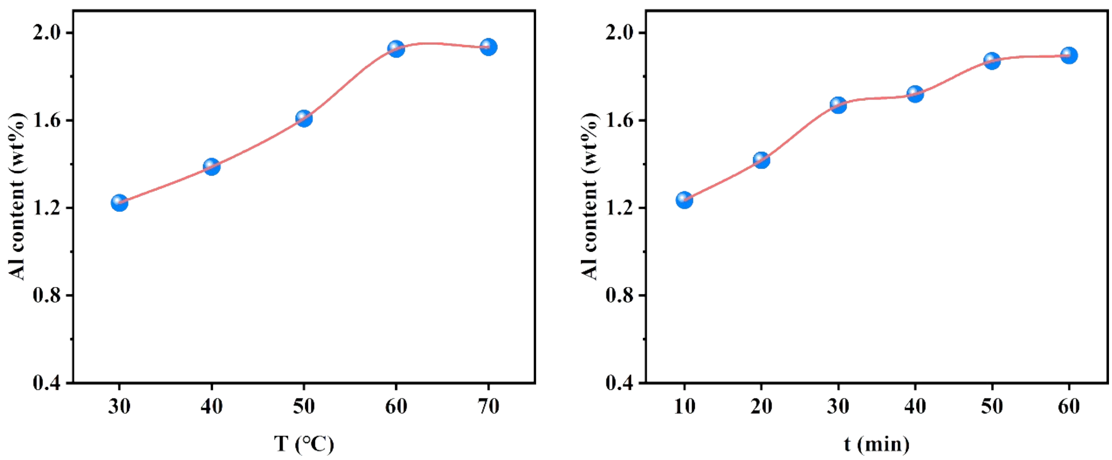

Supplementary Fig. 6 Al content in water solution with different temperatures and time after Al foil-$LiFePO_4$ layer separation operation.

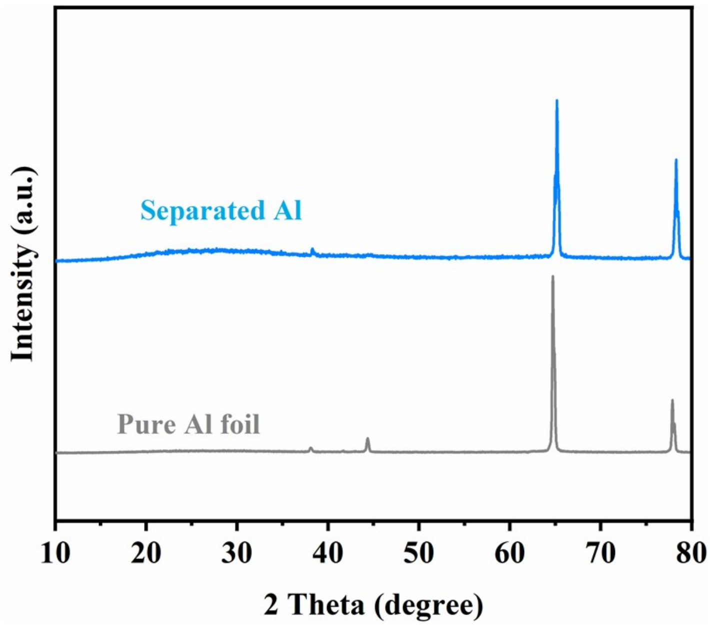

Supplementary Fig. 7 The XRD patterns of the separated and pure Al foil.

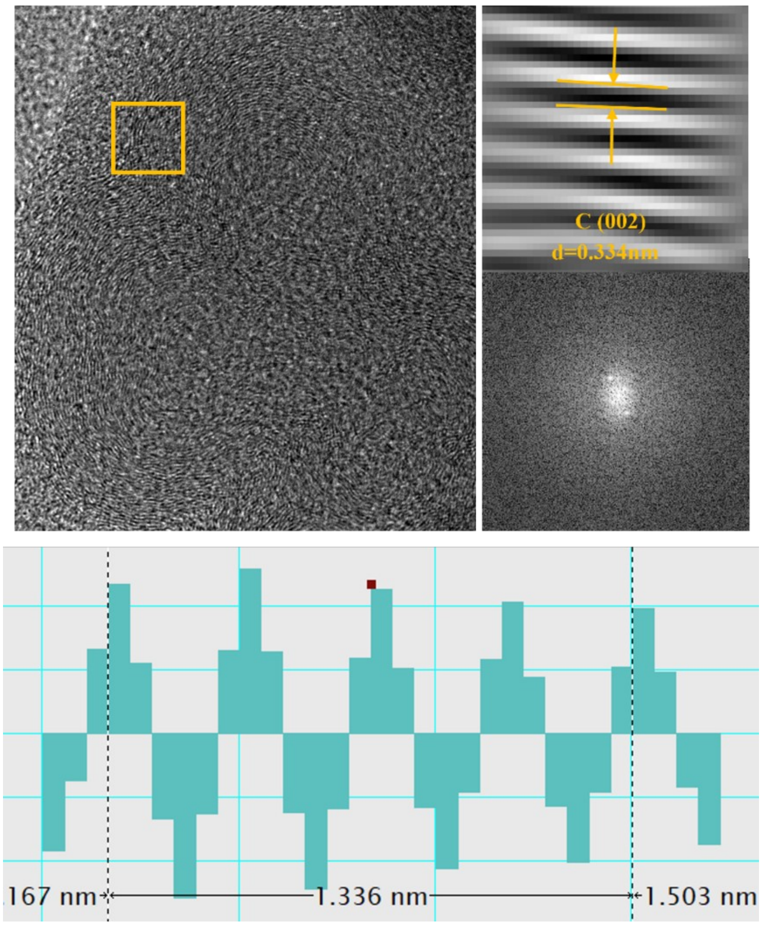

Supplementary Fig. 8 HR-TEM images and the corresponding fast Fourier transform (FFT) images of Da-Gra within the solid rectangle, along with the line intensity profile.

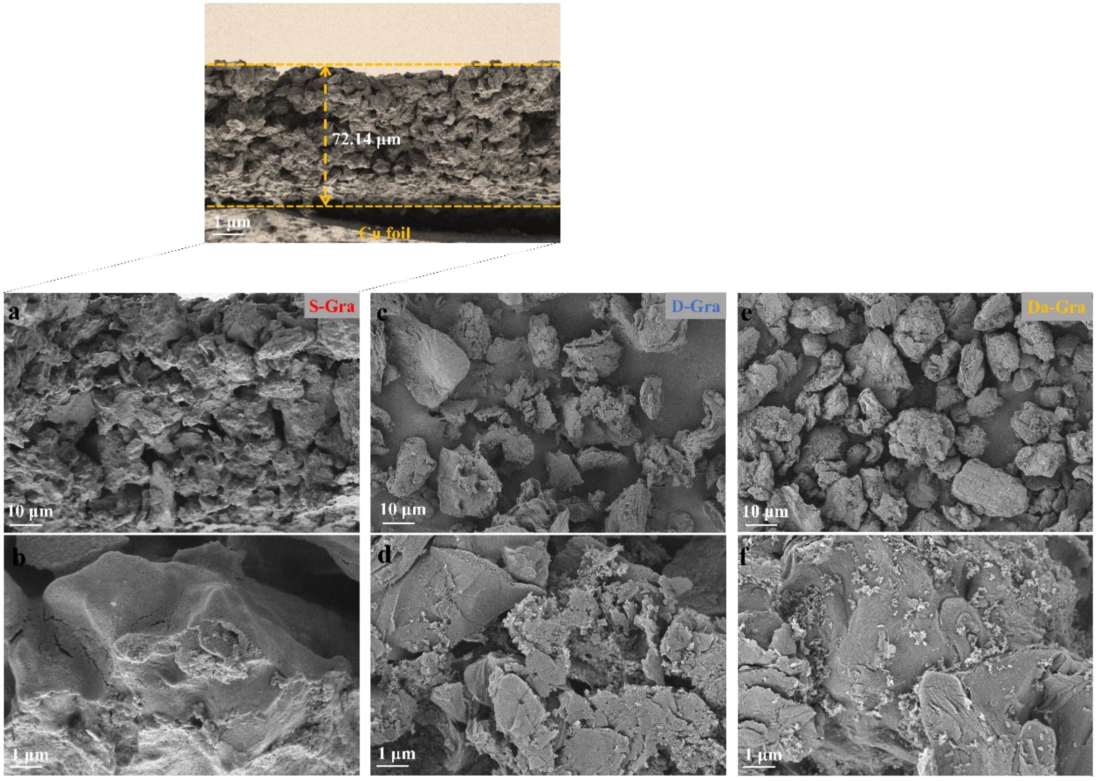

Supplementary Fig. 9 SEM images of different samples at low and high resolutions. (a, b) S-Gra, (c, d) D-Gra, (e, f) Da-Gra.

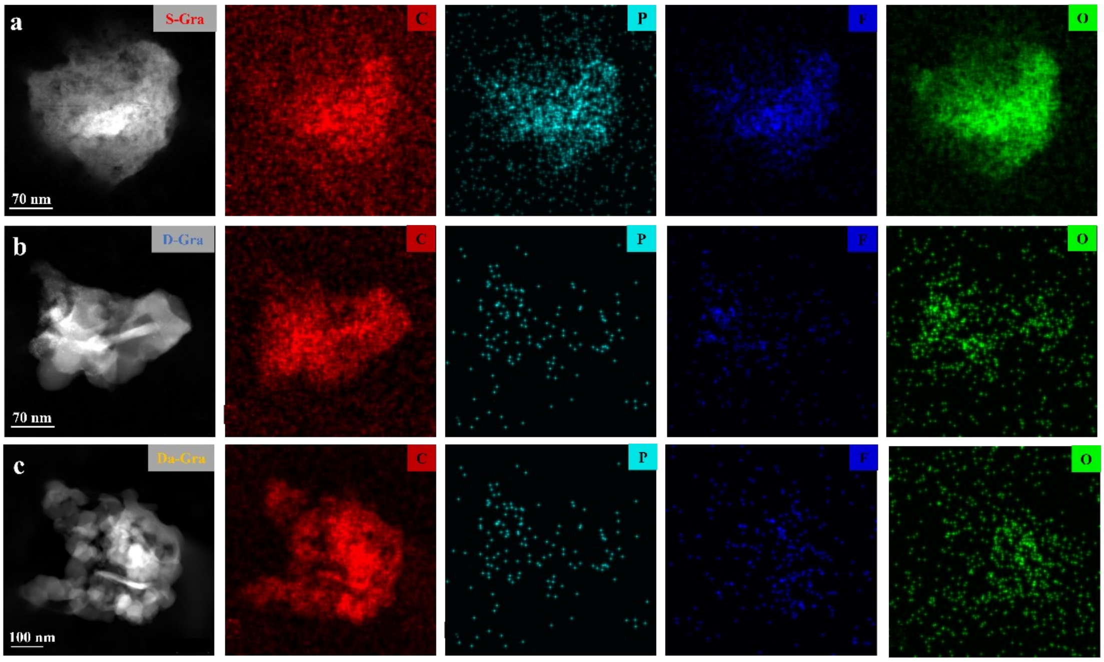

Supplementary Fig. 10 EDS elemental maps of (a) S-Gra, (b) D-Gra and (c) Da-Gra.

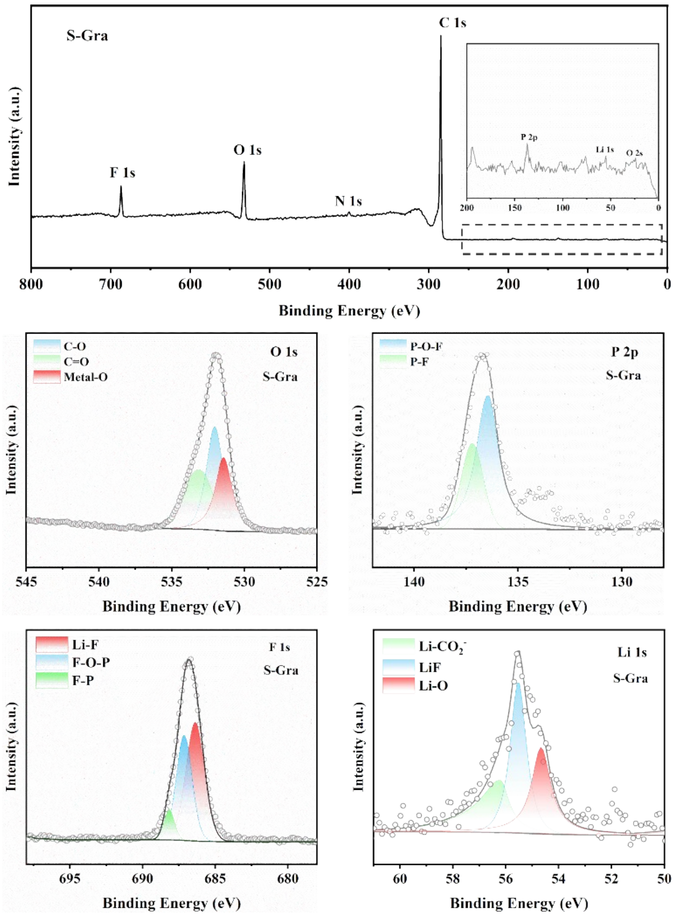

Supplementary Fig. 11 Survey XPS spectrum and high-resolution XPS spectra of O 1s, P 2p, F 1s and Li 1s for S-Gra.

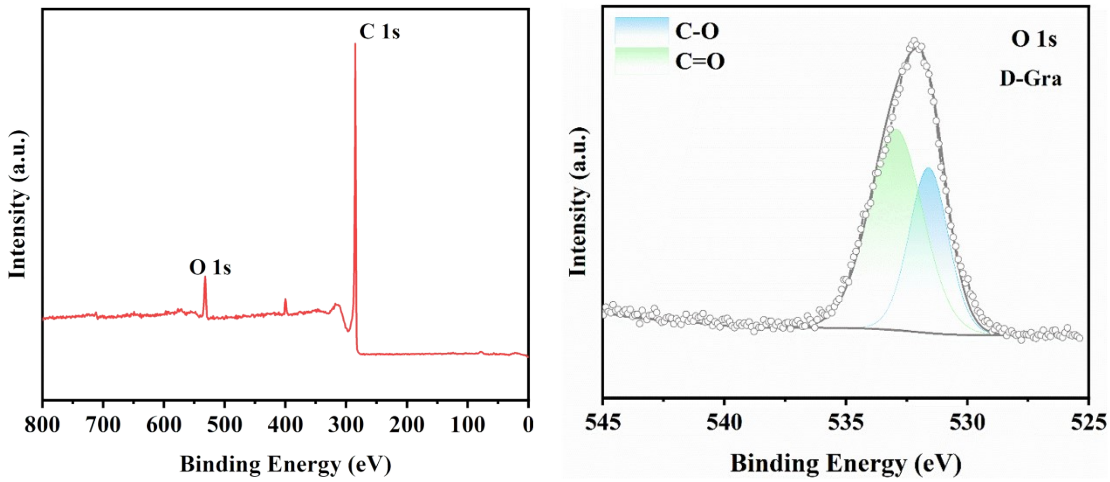

Supplementary Fig. 12 Survey XPS spectrum and high-resolution XPS spectra of O 1s for D-Gra.

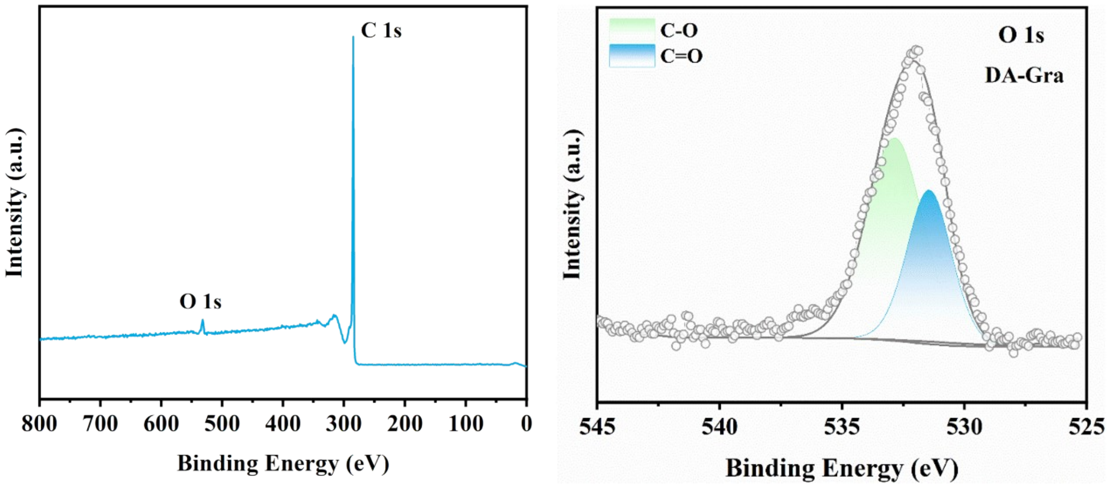

Supplementary Fig. 13 Survey XPS spectrum and high-resolution XPS spectra of O 1s for Da-Gra.

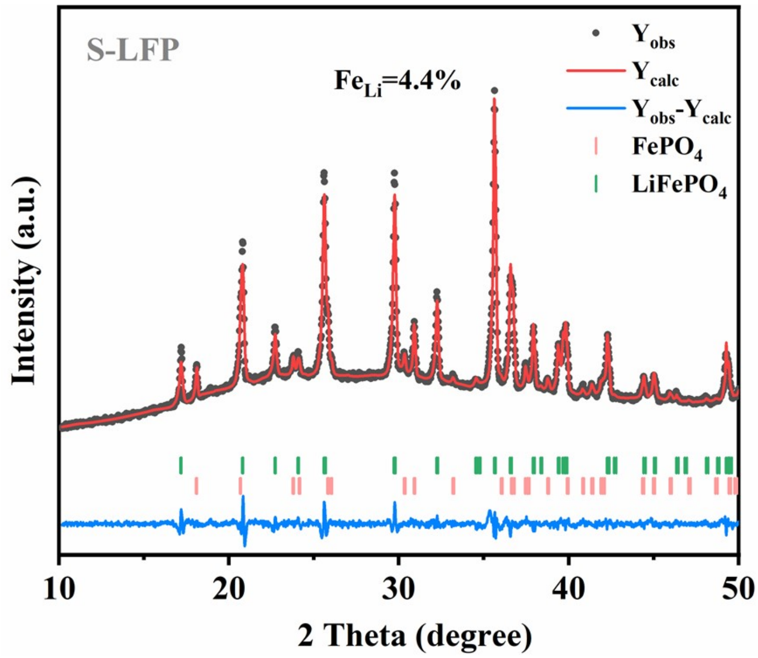

Supplementary Fig. 14 Rietveld refinement of the XRD patterns of S-LFP.

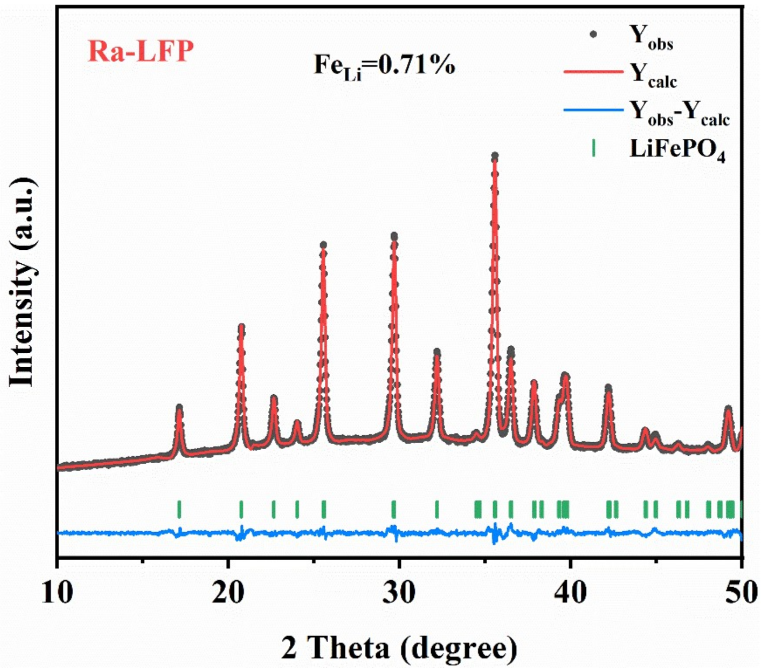

Supplementary Fig. 15 Rietveld refinement of the XRD patterns of Ra-LFP.

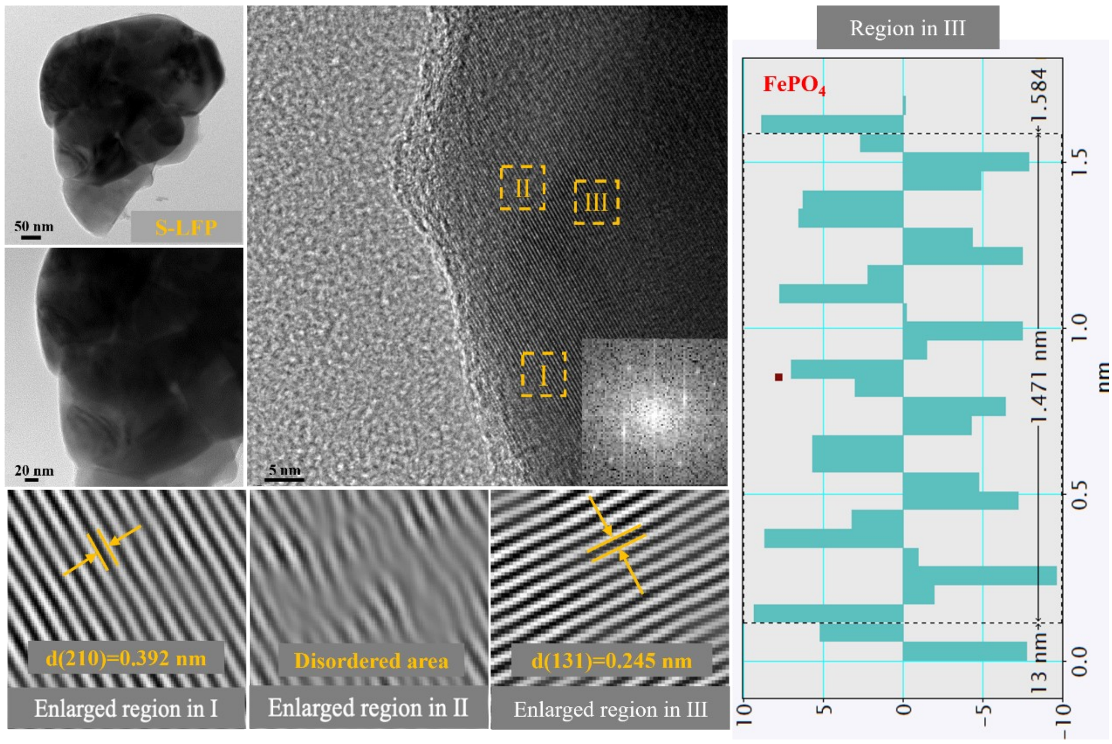

Supplementary Fig. 16 HR-TEM image of the corresponding regions in the dashed rectangles and the corresponding FFT pattern of S-LFP. The lattice spacing analysis of the $FePO_4$ in S-LFP particles.

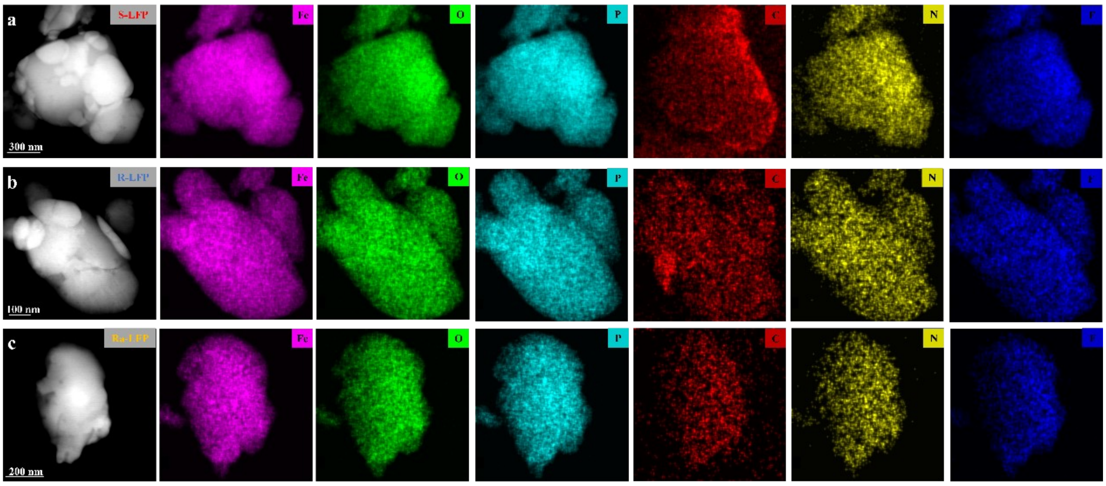

Supplementary Fig. 17 EDS elemental maps of (a) S-LFP, (b) R-LFP and (c) Ra-LFP.

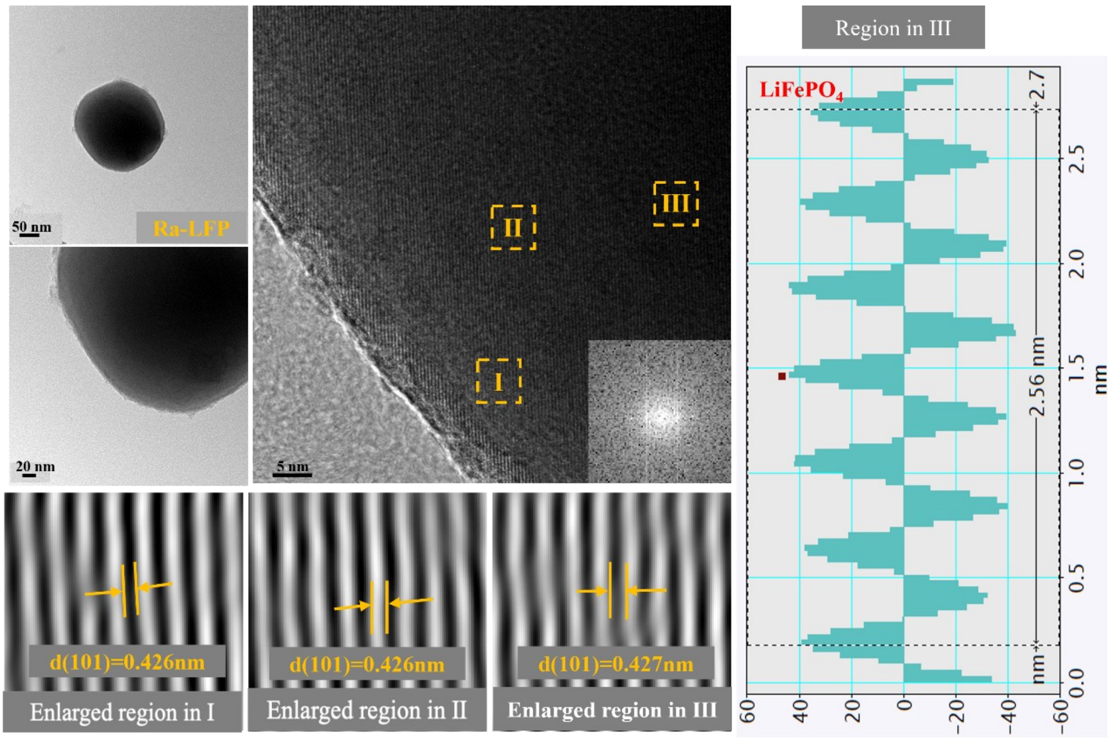

Supplementary Fig. 18 HR-TEM image of the corresponding regions in the dashed rectangles and the corresponding FFT pattern of Ra-LFP. The lattice spacing analysis of the $LiFePO_4$ in Ra-LFP particles.

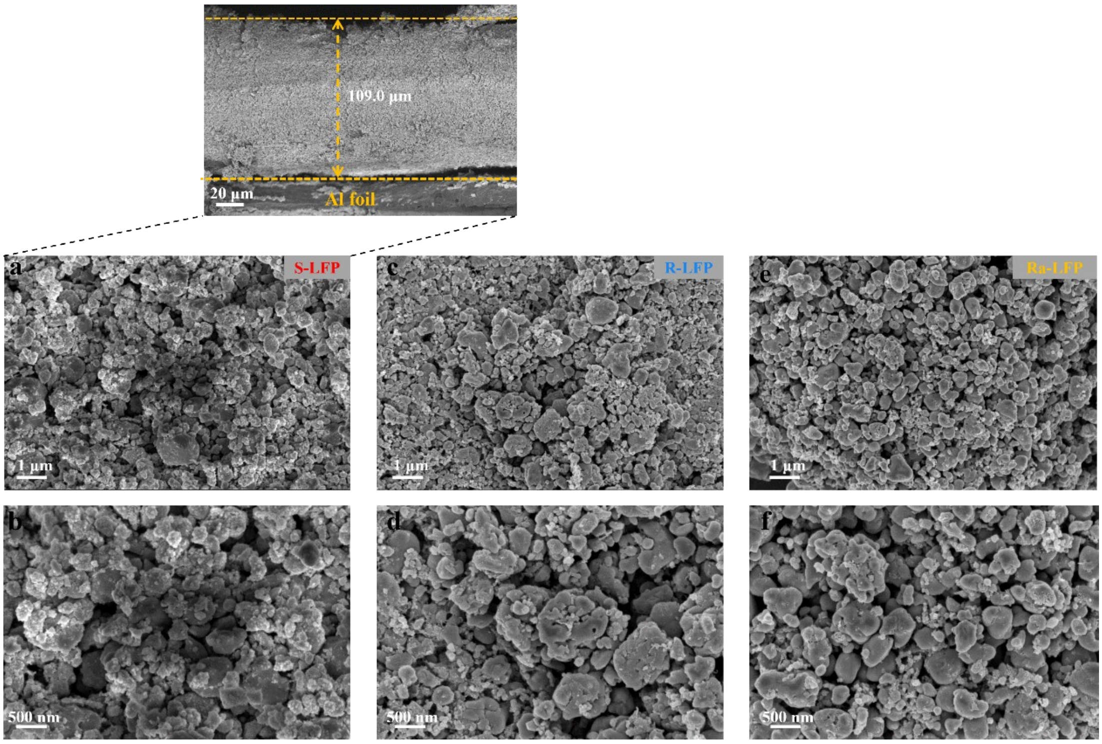

Supplementary Fig. 19 SEM images of different samples at low and high resolutions. (a, b) S-LFP, (c, d) R-LFP, (e, f) Ra-LFP.

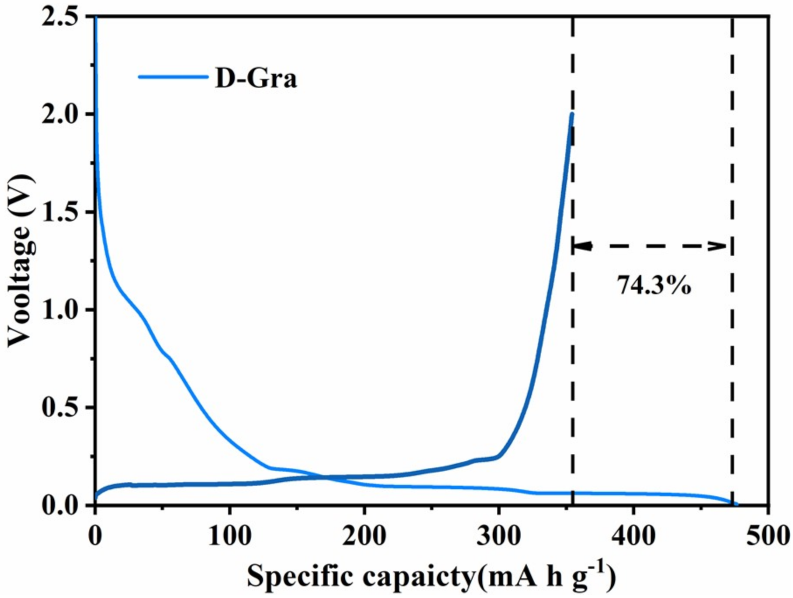

Supplementary Fig. 20 Initial charge and discharge curves of D-Gra at 0.1 C.

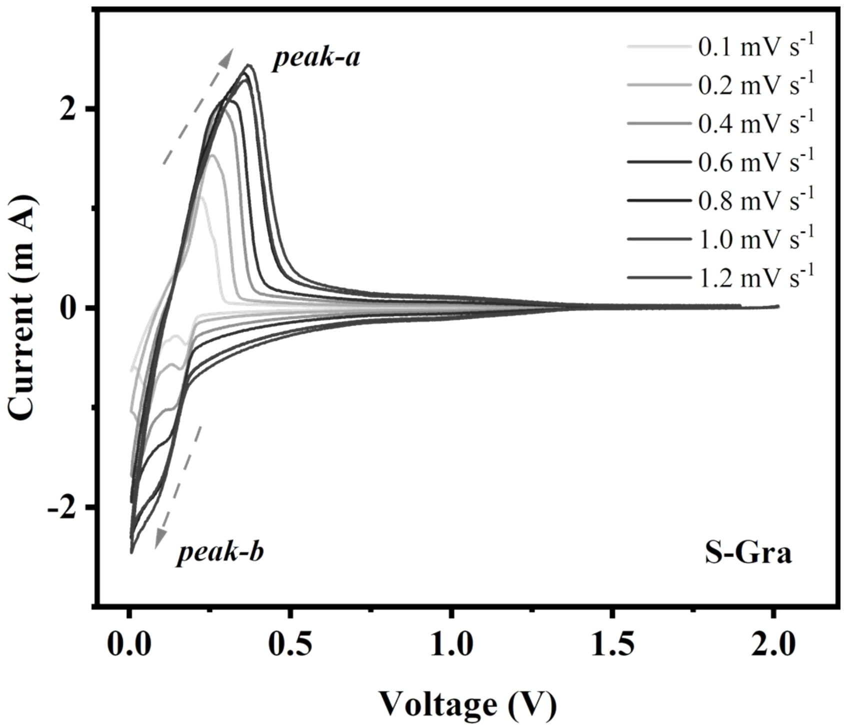

Supplementary Fig. 21 CV curve of S-Gra at different scan rates.

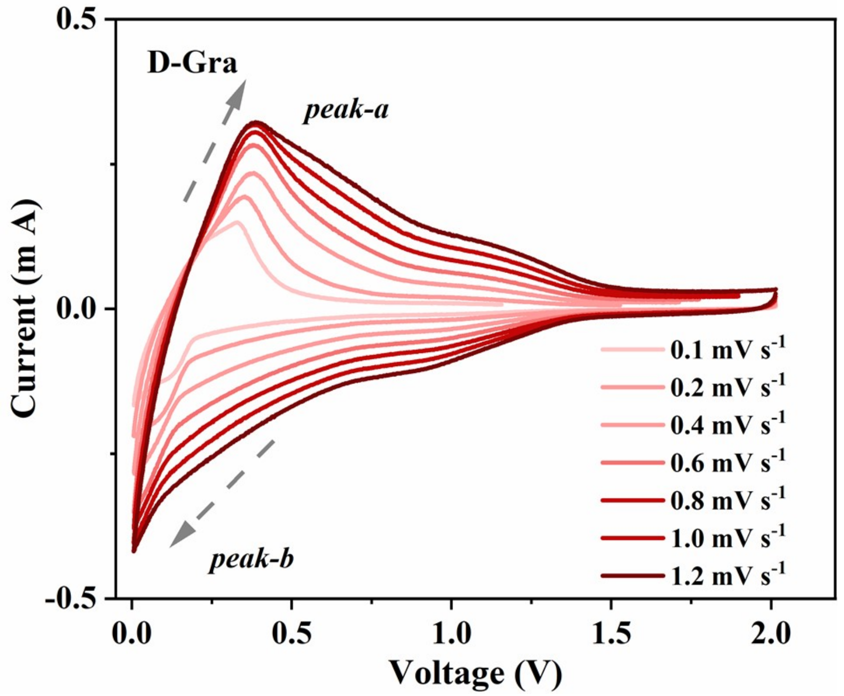

Supplementary Fig. 22 CV curve of D-Gra at different scan rates.

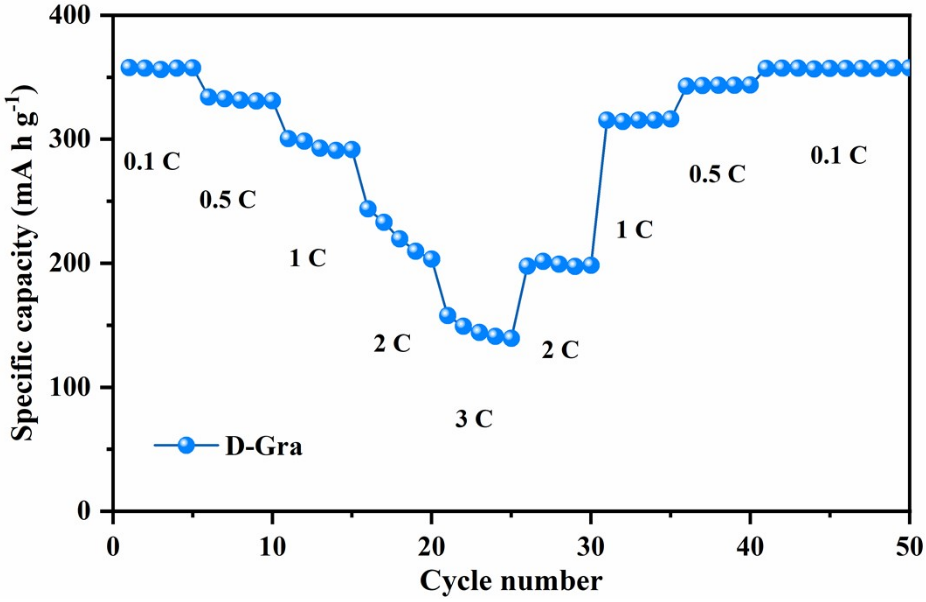

Supplementary Fig. 23 Rate performance of D-Gra.

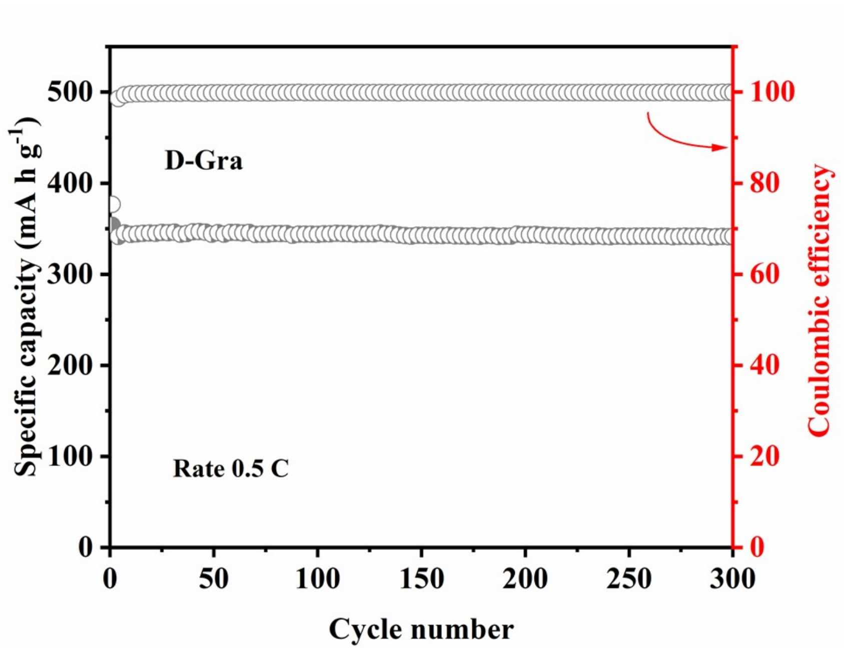

Supplementary Fig. 24 Cycling performance of Da-Gra at 0.5 C.

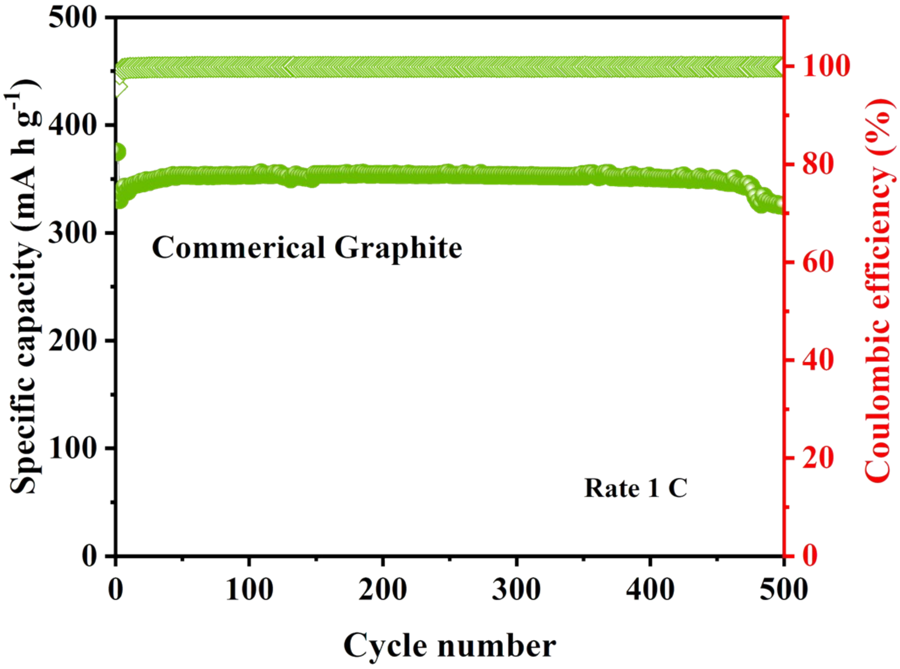

Supplementary Fig. 25 Cycling performance of commercial graphite at 1 C.

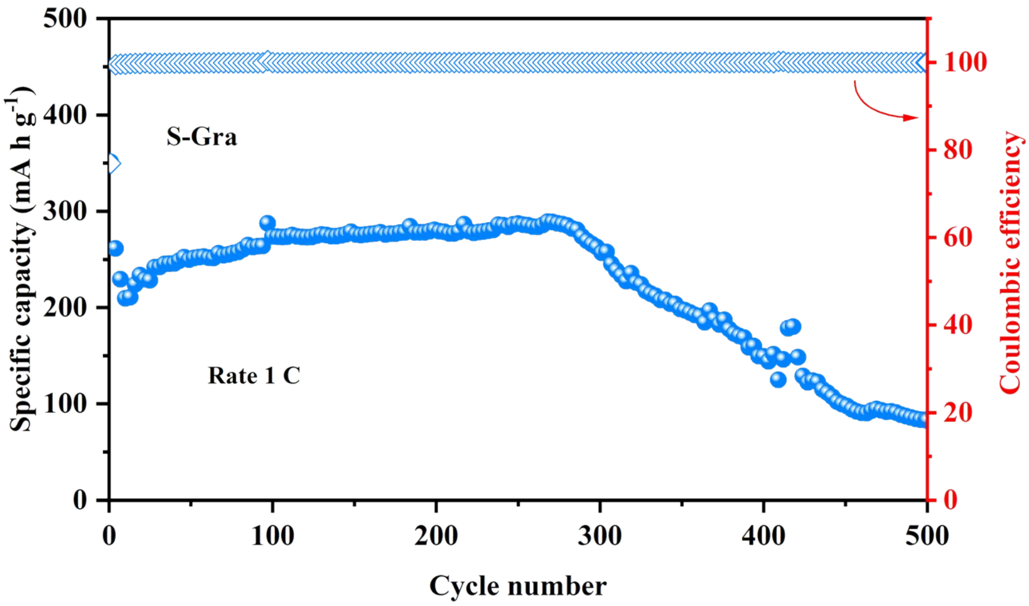

Supplementary Fig. 26 Cycling performance of S-Gra at 1 C.

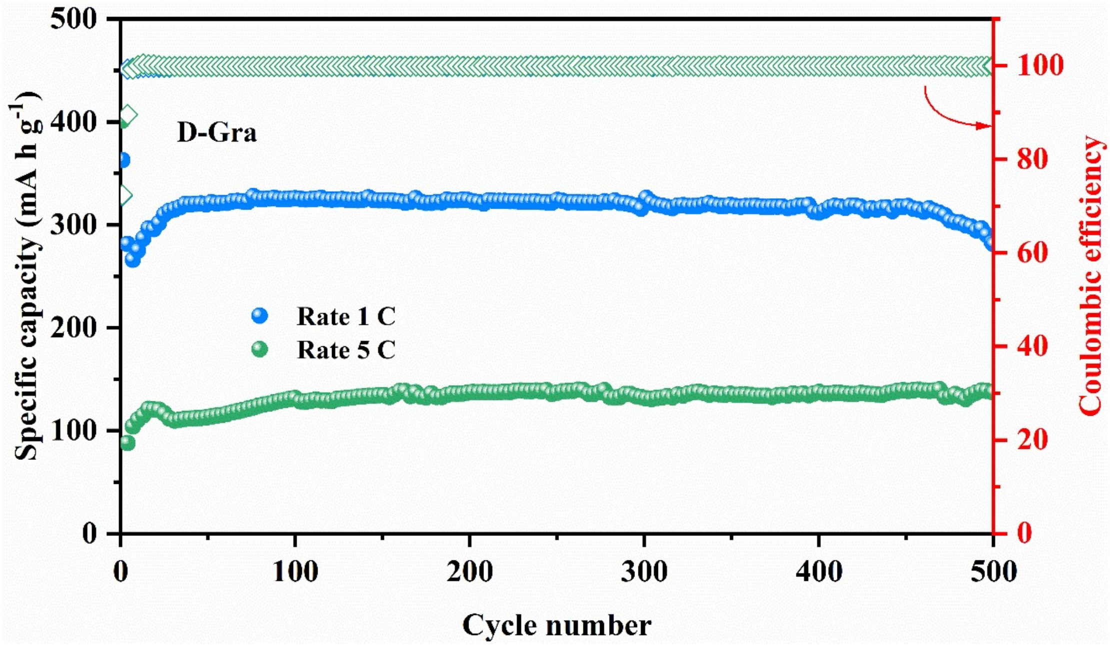

Supplementary Fig. 27 Cycling performance of Da-Gra at 1 and 5 C.

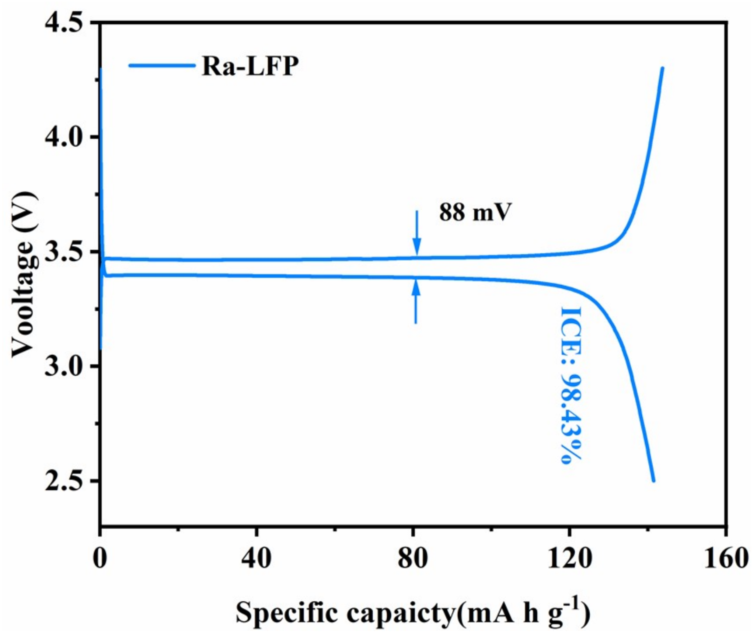

Supplementary Fig. 28 Initial charge and discharge curves of Ra-LFP at 0.1 C.

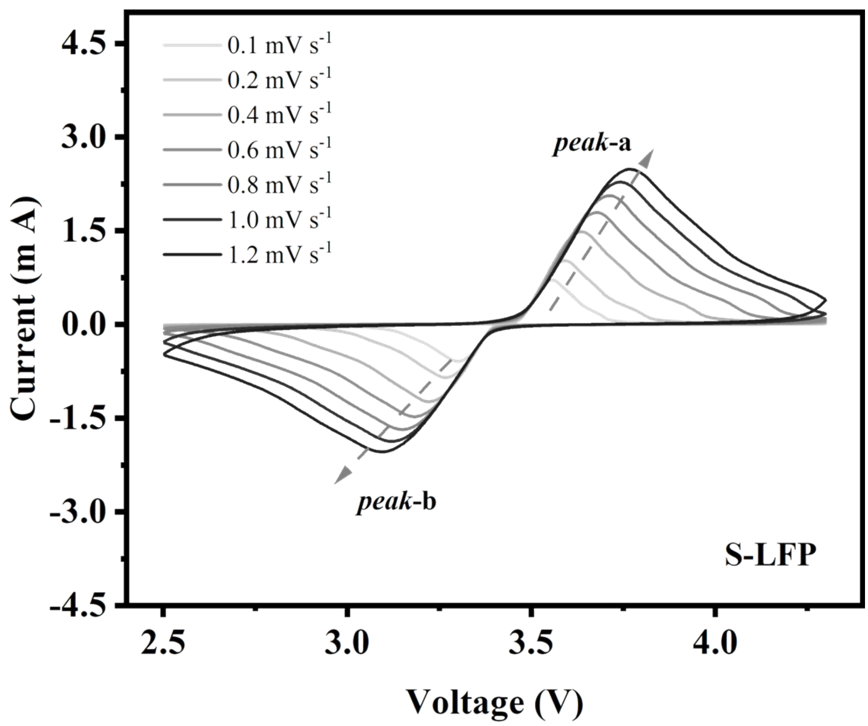

Supplementary Fig. 29 CV curve of S-LFP at different scan rates.

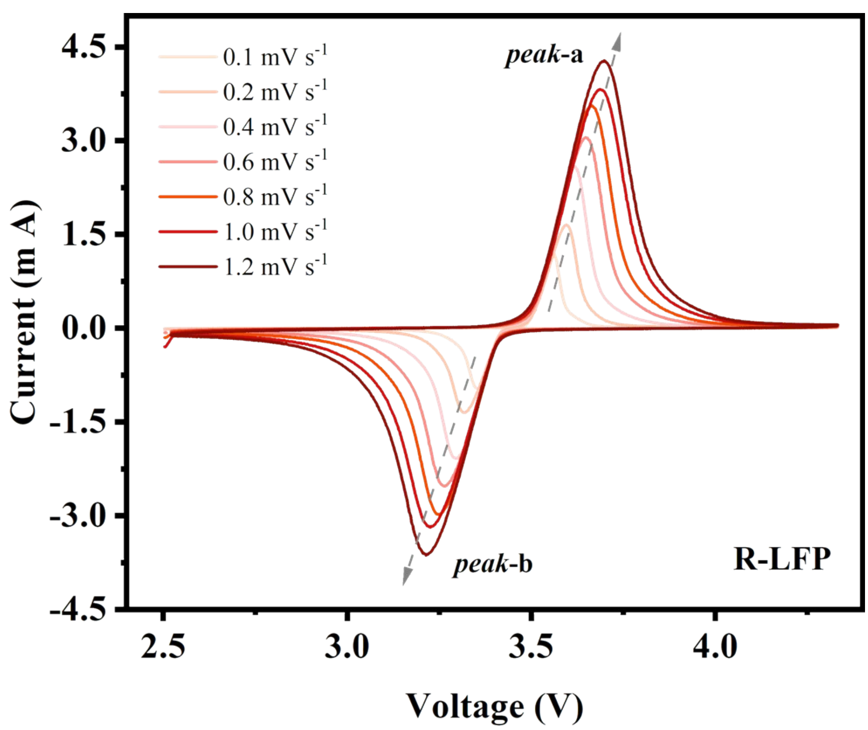

Supplementary Fig. 30 CV curve of R-LFP at different scan rates.

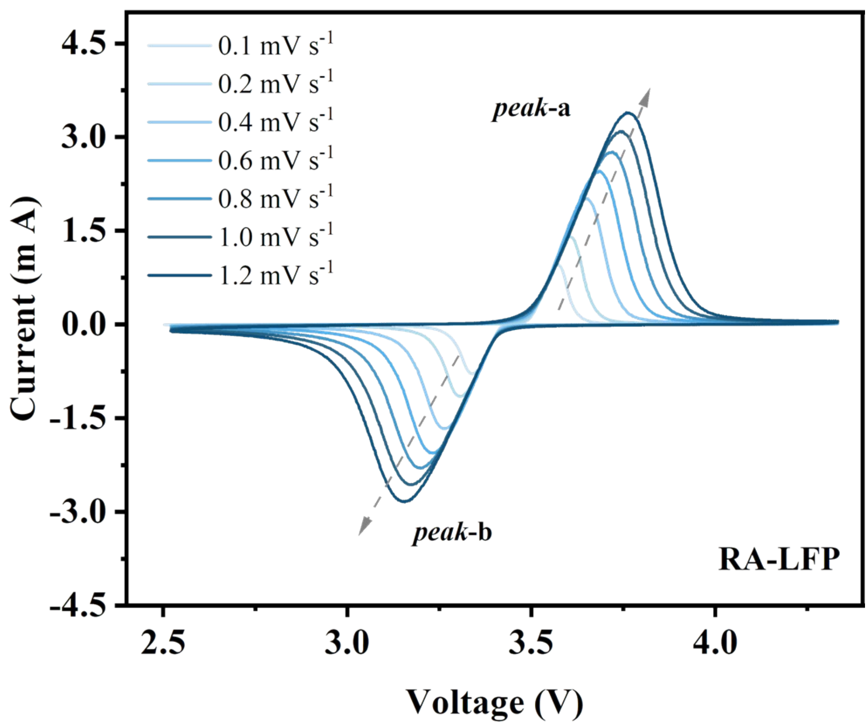

Supplementary Fig. 31 CV curve of Ra-LFP at different scan rates.

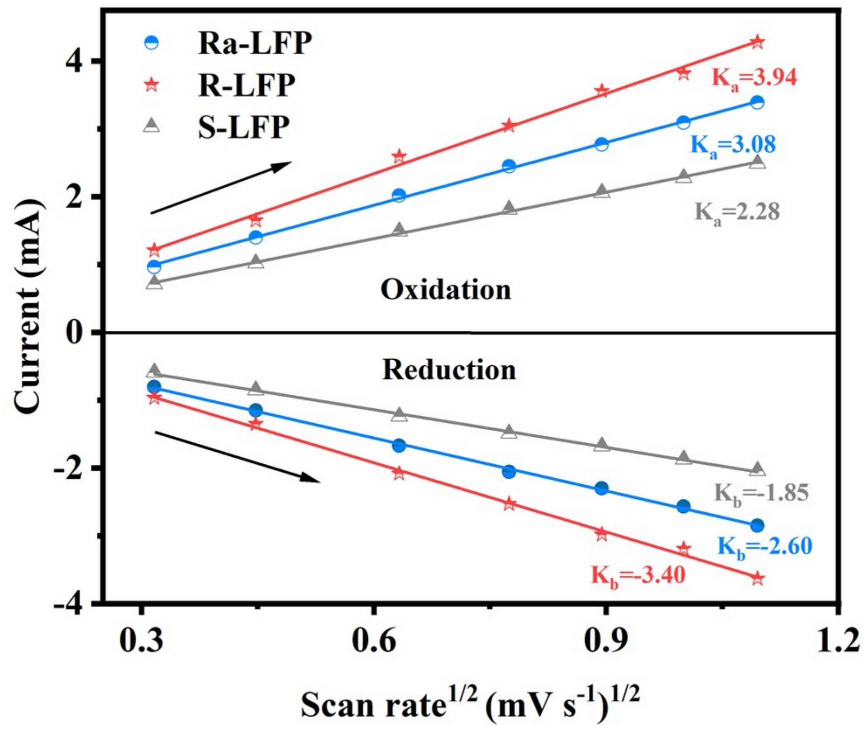

Supplementary Fig. 32 Linear-fitting curves of the major peak currents and scanning rates.

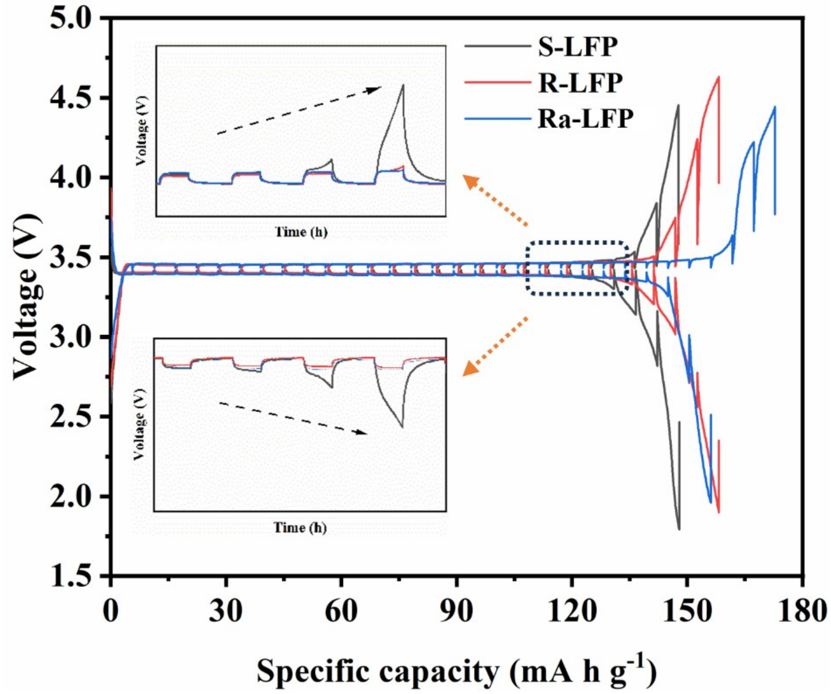

Supplementary Fig. 33 GITT plots of S-LFP, R-LFP and Ra-LFP.

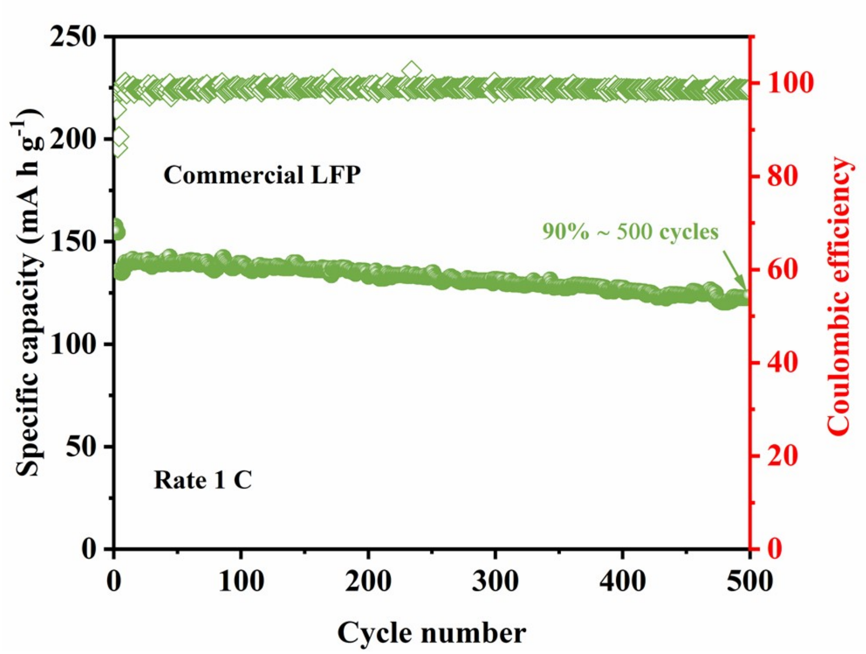

Supplementary Fig. 34 Cycling performance of C-LFP at 1 C.

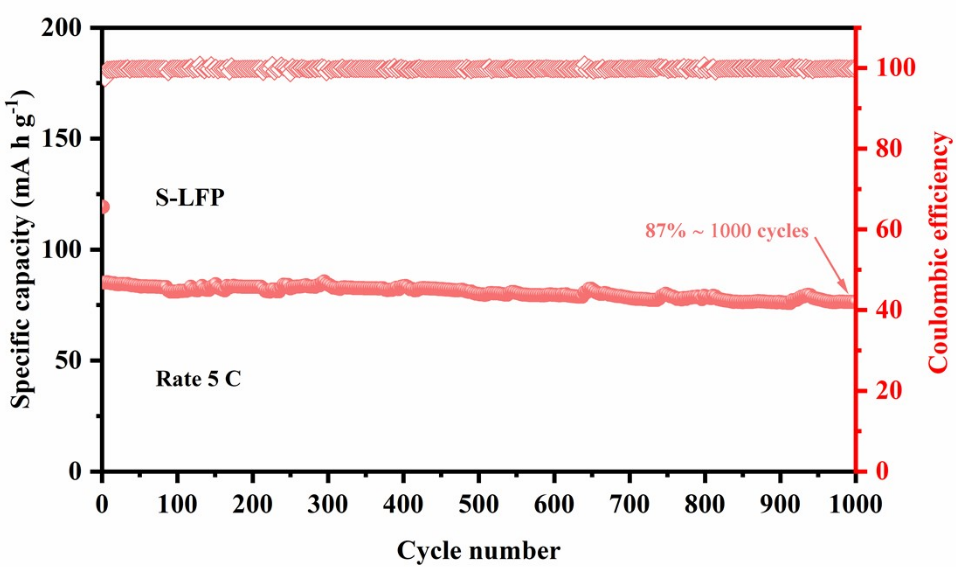

Supplementary Fig. 35 Cycling performance of S-LFP at 5 C.

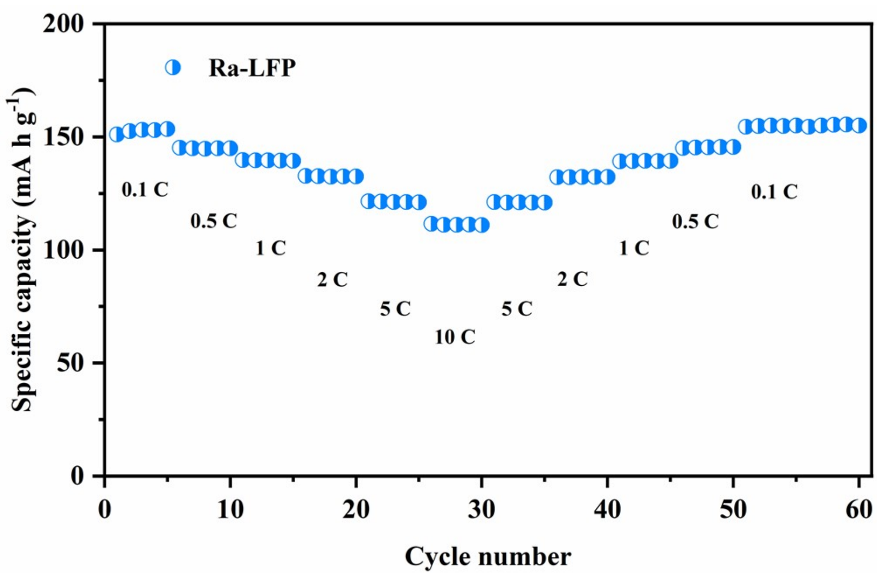

Supplementary Fig. 36 Rate performance of Da-Gra.

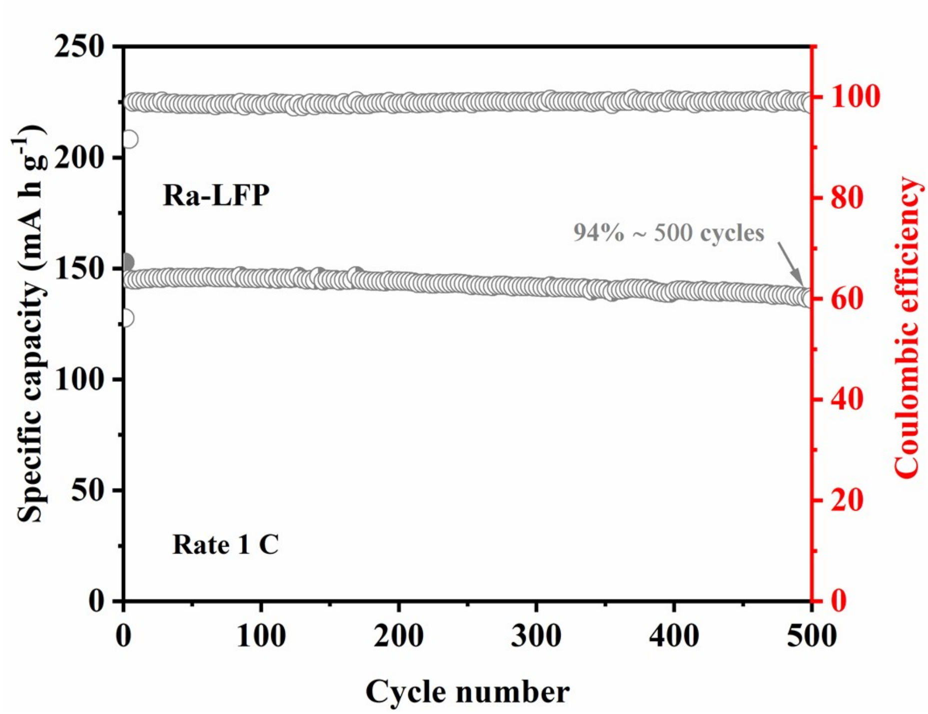

Supplementary Fig. 37 Cycling performance of Ra-LFP at 1 C.

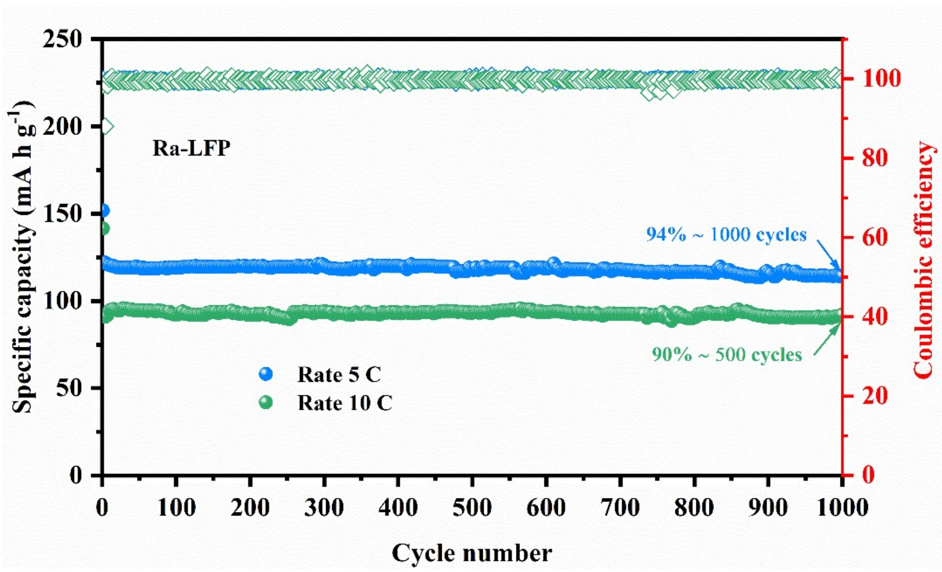

Supplementary Fig. 38 Cycling performance of Ra-LFP at 5 and 10 C.

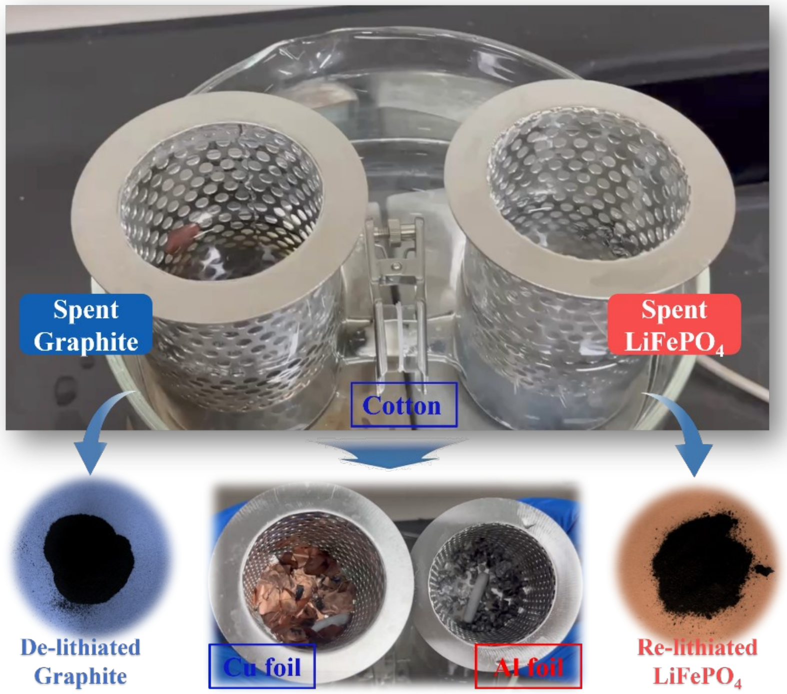

Supplementary Fig. 39 A digital photograph of spent cathode and anode after direct separation and regeneration in the scaled-up Hype cell configuration.

Supplementary Fig. 40 The general and typical processes in different LFPs recycling methods, including pyrometallurgy (Pyro-), hydrometallurgy (Hydro-) and direct (DSR).

Supplementary Table 1. ICP results for Cu contents in water solution at different temperatures and time after Cu foil-graphite layer separation operation.

Temperature (℃)	Cu (mg/L)	Time (min)	Cu (mg/L)
30	0.62	10	0.70
40	0.61	20	0.73
50	0.76	30	0.74
60	0.82	40	0.96
70	0.89	50	0.96
/	/	60	0.97

Supplementary Table 2. ICP results for Li/Fe molar ratio of R-LFP with different lithiation temperatures after diluting 1000 times.

Temperature (℃)	Li (mg/L)	Fe (mg/L)	P (mg/L)
30	0.85	8.17	4.42
40	0.92	8.24	4.43
50	0.96	8.2	4.47
60	1.04	8.69	4.66
70	1.09	4.77	8.91

Supplementary Table 3. ICP results for Li/Fe molar ratio of R-LFP with different pH values after diluting 1000 times.

pH	Li (mg/L)	Fe (mg/L)	P (mg/L)
8	1.02	8.79	4.72
8.5	1.05	8.92	4.79
9	1.03	8.69	4.65
9.5	1.09	8.91	4.77

Supplementary Table 4. ICP results for Li/Fe molar ratio of R-LFP with different lithiation time after diluting 1000 times.

time	Li (mg/L)	Fe (mg/L)	P (mg/L)
10	1.01	8.54	4.57
20	1.03	8.73	4.71
30	1.06	8.95	4.71
40	1.08	9.14	4.78
50	1.06	8.81	4.68
60	1.09	8.91	4.77

Supplementary Table 5. ICP results for Al contents in water solution at different temperatures and time after Al foil- $LiFePO_4$ layer separation operation.

Temperature (℃)	Al (mg/L)		Time (min)	Al (mg/L)
30	0.13		10	0.13
40	0.15		20	0.15
50	0.17		30	0.18
60	0.21		40	0.19
70	0.22		50	0.20
/	/		60	0.21

Supplementary Table 6. Structural parameters obtained from Rietveld refinement of the XRD pattern of S-LFP. **Phase 1 $LiFePO_4$:** Space group: *Pnma*, a=10.327364 Å, b=6.005226 Å, c=4.690605 Å, α=β=γ=90°. **Phase 2 $FePO_4$:** Space group: *Pnma*, a=9.809450 Å, b=5.786042 Å, c=4.779844 Å, α=β=γ=90°.

Atoms	**Site**	**Wyckoff positions**			**Occupancy**	**Site**	**Wyckoff positions**			**Occupancy**
Li	4a	0	0	0	0.95598	NA				
Fe	4a	0	0	0	0.04402	4a	0.00000	0.00000	0.00000	0.01200
Fe	4c	0.28136	0.25000	0.97040	0.95598	4c	0.27211	0.25000	0.94679	0.98800
Li	4c	0.28136	0.25000	0.97040	0.04402	NA				
P	4c	0.09424	0.25000	0.41413	1	4c	0.09546	0.25000	0.37701	1
O	4c	0.09725	0.25000	0.73635	1	4c	0.11840	0.25000	0.71821	1
O	4c	0.44984	0.25000	0.19902	1	4c	0.43774	0.25000	0.16289	1
O	8d	0.16375	0.04192	0.28121	1	8d	0.1676	0.06044	0.24428	1

Supplementary Table 7. Structural parameters obtained from Rietveld refinement of the XRD pattern of R-LFP. **Phase $LiFePO_4$:** Space group: *Pnma*, a=10.322839 Å, b=6.001675 Å, c=4.687203 Å, α=β=γ=90°.

Atoms	**Site**	**Wyckoff positions**			**Occupancy**
Li	4a	0	0	0	0.99154
Fe	4a	0	0	0	0.00846
Fe	4c	0.28163	0.25000	0.97251	0.99154
Li	4c	0.28163	0.25000	0.97251	0.00846
P	4c	0.09558	0.25000	0.42261	1
O	4c	0.09015	0.25000	0.74942	1
O	4c	0.45244	0.25000	0.21473	1
O	8d	0.15987	0.04707	0.28457	1

Supplementary Table 8. Structural parameters obtained from Rietveld refinement of the XRD pattern of Ra-LFP. **Phase $LiFePO_4$:** Space group: *Pnma*, a=10.346512 Å, b=6.016788 Å, c= 4.700098Å, α=β=γ=90°.

Atoms	**Site**	**Wyckoff positions**			**Occupancy**
Li	4a	0	0	0	0.99286
Fe	4a	0	0	0	0.00714
Fe	4c	0.28267	0.25000	0.97510	0.99286
Li	4c	0.28267	0.25000	0.97510	0.00714
P	4c	0.09278	0.25000	0.42706	1
O	4c	0.08867	0.25000	0.75660	1
O	4c	0.44914	0.25000	0.22520	1
O	8d	0.16091	0.05684	0.28491	1

Supplementary Table 9. The discharge capacity resulting from the direct recycling of published articles varies at different rates.

No.	0.1 C	0.2 C	0.5 C	1 C	2 C	5C	10 C	Ref.
S1	151.3	148.7	146.6	141.3	132.2	113.1	92.4	1
S2	/	/	/	140.1	131.6	112.8	93.0	2
S3	/	/	143	140	134	117	/	3
S4	/	150.9	140	125.7	110.1	89.2	71.3	4
S5	/	/	138	/	/	/	/	5
S6	151.1	/	142.8	134.8	123	104.2	87.9	6
S7	/	/	/	139.2	131.2	116	105.5	7
S8	/	/	/	147.9	136.1	113.6	87.2	8
S9	157	/	/	/	127	111	97	9
S10	/	/		139.1	/	/	100.1	10
S11	148.7	/	143.6	135.4	123.3	102.5	/	11
S12	156.6	/	151.8	145.9	/	122.1	/	12

Supplementary Table 10 Basic data of techno-economic analysis by Hydro- and DSR recycling.

No.	Item	Market price	Unit	Update Data	Data Sources
1	Spent LFP (pouch cell)	8000	¥ t^{-1}	Dce. 27th 2024	SMM
2	Li_2CO_3	75400	¥ t^{-1}	Dce. 27th 2024	SMM
3	LiOH	69798	¥ t^{-1}	Dce. 27th 2024	SMM
4	Na_2CO_3	3000	¥ t^{-1}	Dce. 27th 2024	100PPI
5	H_2SO_4 (98%)	380	¥ t^{-1}	Dce. 27th 2024	100PPI
6	H_2O_2 (27.5%)	1800	¥ t^{-1}	Dce. 27th 2024	100PPI
7	$NaSO_3$	2800	¥ t^{-1}	Dce. 27th 2024	100PPI
8	Ar	2400	¥ t^{-1}	Dce. 27th 2024	100PPI
9	Electricity	0.61	¥ $kW \cdot h^{-1}$	Dce. 27th 2024	ZZJSJ
10	Water	2.96	¥ t^{-1}	Dce. 27th 2024	ZZJSJ
11	Average labor cost	73000	¥ a^{-1}	Dce. 27th 2024	DOI: 10.1038/s41467-023-36197-6
12	Sewage Treatment	40	¥ t^{-1}		
13	$LiFePO_4$ cathode material	37510	¥ t^{-1}	Dce. 27th 2024	SMM

a) 1$ = 7.2985 ¥ (Update time: 2024/12/27);

b) SMM (https://www.smm.cn/), 100PPI (https://www.100ppi.com/ppi/), ZZJSJ (https://zzjsj.zhengzhou.gov.cn/).

Supplementary Table 11 Cost analysis of hydro- recycling strategy.

Cost analysis based on hydrometallurgical recovery							
Main	No.	Item	Unit Price (¥ t^{-1})	Dose (t)	Note	Data Sources	Cost (¥)
Raw material	1	Spent LFP battery	8000	1.00	250 kg of spent LFP can be sorted from per 1 ton of spent battery	DOI: 10.1002/adma.202414048	8000
	Subtotal (¥)						**8000**
Main	No.	Item	Unit Price (¥ t^{-1})	Dose (t)	Note	Data Sources	Cost (¥)
Reagent	2	H_2SO_4	380	0.0885	Leaching agent	DOI:10.1021/acssuschemeng.7b01594	33.63
	3	H_2O_2	1800	0.1116	Oxidating agent		200.88
	4	Na_2CO_3	3000	0.0541	Precipitating agent		162.3
	Subtotal (¥)						**396.81**
Main	No.	Item	Unit Price (¥ t^{-1})	Dose (t)	Note	Data Sources	Cost (¥)
Average labor	5	Disassembly	73000	0.01		DOI. 10.1016/j.xcrp.2022.100741	730
	6	Recycling step	73000	0.02			1460
	Subtotal (¥)						**2190**
Main	No.	Item	Unit Price (¥ t^{-1} /¥ k Wh)	Dose (t/k Wh)	Note	Data Sources	Cost (¥)
Electricity & water	7	Electricity	0.61	500		DOI:10.1038/s41467-023-36197-6	305
	8	Water	2.96	500			1480
	Subtotal (¥)						**1785**
Main	No.	Item	Unit Price (¥ t^{-1})	Dose (t)	Note	Data Sources	Cost (¥)
Equipment depreciation	9	Equipment depreciation	5000	0.25		DOI: 10.3969/j.issn.1009-847X.2018.10.006	1250
	Subtotal (¥)						**1250**
Main	No.	Item	Unit Price (¥ t^{-1})	Dose (t)	Note	Data Sources	Cost (¥)
Sewage treatment	10	Sewage treatment	40	20		DOI: 10.3969/j.issn.1009-847X.2018.10.006	800
	Subtotal (¥)						**800**
Total Cost (¥)							***14421.81***
In table S6, the cost per one ton of spent LFP battery was calculated using the hydro-route. The recycling process can be divided into three steps: disassembling the spent battery, separating cathode active materials and subsequently conducting hydro-leaching to extract lithium. It is assumed that the level of deficiency in the spent LFP battery remains consistent ($Li_{0.8}FePO_4$) based on hydro- recovery, DSR and hydro- synthesized methods.							

Supplementary Table 12 Cost analysis of hydro- and re-synthesized recovery strategy.

Cost analysis based on hydrometallurgical and re-synthesized recovery strategy							
Main	No.	Item	Unit Price (¥ t^{-1})	Dose (t)	Note	Data Sources	Cost (¥)
Raw material	1	Spent LFP battery	8000	1.00	250 kg of spent LFP can be sorted from per 1 ton of spent battery	DOI: 10.1002/adma.202414048	8000
	Subtotal (¥)						**8000**
Main	No.	Item	Unit Price (¥ t^{-1})	Dose (t)	Note	Data Sources	Cost (¥)
Reagent	2	H_2SO_4	380	0.0885	Leaching agent	DOI: 10.1016/j.cej.2023.147201 DOI:10.1021/acssuschemeng.7b01594 DOI: 10.1039/D1TA07757K	33.63
	3	H_2O_2	1800	0.1116	Oxidating agent		200.88
	4	Na_2CO_3	3000	0.0541	Precipitating agent		162.3
	5	Li_2CO_3	75400	0.0146	Used as the supplement of lithium during the annealing process		1100.84
	6	Ar	2400	0.03	Used as the protective atmosphere during regeneration process		72
	Subtotal (¥)						**1569.65**
Main	No.	Item	Unit Price (¥ t^{-1})	Dose (t)	Note	Data Sources	Cost (¥)
Average labor	7	Disassembly	73000	0.01		DOI. 10.1016/j.xcrp.2022.100741	730
	8	Recycling & synthesized	73000	0.03			2190
	Subtotal (¥)						**2920**
Main	No.	Item	Unit Price (¥ t^{-1} /¥ k Wh)	Dose (t/k Wh)	Note	Data Sources	Cost (¥)
Electricity & water	9	Electricity	0.61	800		DOI:10.1038/s41467-023-36197-6	488
	10	Water	2.96	500			1480
	Subtotal (¥)						**1968**
Main	No.	Item	Unit Price (¥ t^{-1})	Dose (t)	Note	Data Sources	Cost (¥)
Equipment depreciation	11	Equipment depreciation	5000	0.25		DOI: 10.3969/j.issn.1009-847X.2018.10.006	1250
	Subtotal (¥)						**1250**
Main	No.	Item	Unit Price (¥ t^{-1})	Dose (t)	Note	Data Sources	Cost (¥)
Sewage treatment	12	Sewage treatment	40	20		DOI: 10.3969/j.issn.1009-847X.2018.10.006	800
	Subtotal (¥)						**800**
Total Cost (¥)							***16507.65***
In table S6, the cost per one ton of spent LFP battery was calculated using the hydro-route. The recycling process can be divided into three steps: disassembling the spent battery, separating cathode active materials and subsequently conducting hydro-leaching to extract lithium. It is assumed that the level of deficiency in the spent LFP battery remains consistent ($Li_{0.8}FePO_4$) based on hydro- recovery, DSR and hydro- synthesized methods.							

Supplementary Table 13 Cost analysis of DSR recycling strategy.

Cost analysis based on direct separation and regeneration strategy							
Main	No.	Item	Unit Price (¥ t^{-1})	Dose (t)	Note	Data Sources	Cost (¥)
Raw material	1	Spent LFP battery	8000	1.00	310 kg of spent LFP electrode can be sorted from per 1 ton of spent battery	DOI: 10.1002/adma.202414048	8000
	Subtotal (¥)						**8000**
Main	No.	Item	Unit Price (¥ t^{-1})	Dose (t)	Note	Data Sources	Cost (¥)
Reagent	2	$NaSO_3$	2800	0.0399	Used as reductant in the re-lithiation process	DOI: 10.1016/j.cej.2023.147201 DOI: 10.1016/j.joule.2020.10.008 DOI: 10.1021/acsenergylett.3c02256	351.92
	3	LiOH	69798	0.0061	Used as lithium salt to re-lithiate the spent LFP		425.77
	4	Li_2CO_3	75400	0.0017	Used as the supplement of volatile lithium during the short annealing process		128.18
	5	Ar	2400	0.015	Used as the protective atmosphere during regeneration process		36
	Subtotal (¥)						**941.87**
Main	No.	Item	Unit Price (¥ t^{-1})	Dose (t)	Note	Data Sources	Cost (¥)
Average labor	6	Disassembly & Recovery	73000	0.02		DOI. 10.1016/j.xcrp.2022.100741	1460
	Subtotal (¥)						**1460**
Main	No.	Item	Unit Price (¥ t^{-1} /¥ k Wh)	Dose (t/k Wh)	Note	Data Sources	Cost (¥)
Electricity & water	7	Electricity	0.61	200		DOI:10.1038/s41467-023-36197-6	122
	8	Water	2.96	300		DOI: 10.3969/j.issn.1009-847X.2018.10.006	888
	Subtotal (¥)						**1010**
Main	No.	Item	Unit Price (¥ t^{-1})	Dose (t)	Note	Data Sources	Cost (¥)
Equipment depreciation	9	Equipment depreciation	5000	0.25		DOI: 10.3969/j.issn.1009-847X.2018.10.006	1250
	Subtotal (¥)						**1250**
Main	No.	Item	Unit Price (¥ t^{-1})	Dose (t)	Note	Data Sources	Cost (¥)
Sewage treatment	10	Sewage treatment	40	10		DOI: 10.3969/j.issn.1009-847X.2018.10.006	400
	Subtotal (¥)						**400**
Total Cost (¥)							***13061.87***
In table S7, the cost per one ton of spent LFP battery was calculated using the DSR route. The recycling process can be divided into three steps: disassembling the spent battery, separating electrode and subsequently conducting direct re-lithiation to replenish lithium. It is assumed that the level of deficiency in the spent LFP battery remains consistent ($Li_{0.8}FePO_4$) based on hydro- recovery and DSR methods.							

Supplementary Table 14 Hydro- recovery revenue analysis.

Revenue analysis based on hydro- recovery								
No.	Item	Material	Recovery yield (%)	Production (t)	Market price (¥ t^{-1})	Revenue (¥)	Update Date	Data Sources
1	Lithium salt	Li_2CO_3	95	0.0446	75400	3362.84	Dce. 27th 2024	SMM
2	Precursor	$FePO_4$	95	0.227	10600	2406.2	Dce. 27th 2024	SMM
3	Anode	Graphite	96	0.125	20400	2550	Dce. 27th 2024	SMM
4	Current collector	Al foil	90	0.0540	35200	1900.8	Dce. 27th 2024	SMM
5	Current collector	Cu foil	90	0.090	92420	8317.8	Dce. 27th 2024	Mysteel
Subtotal (¥) ***18537.64***								
Note: a) It is assumed that the level of deficiency in the spent LFP battery remains consistent ($Li_{0.8}FePO_4$) based on hydro- recovery and DSR methods. b) The proportion of each component is 25% of cathode material, 13% of graphite, 6% of Al foil, 10% of Cu foil, 3% of separator, 16% of electrolyte, and 20% of shell. c) The value of separator, electrolyte, and shell is hard to assess in the real process, therefore, these components are excluded from the revenue analysis. d) Mysteel (https://www.mysteel.com/).								

Supplementary Table 15 Hydro- and re-synthesized recovery revenue analysis.

Revenue analysis based on hydro- recovery								
No.	Item	Material	Recovery yield (%)	Production (t)	Market price (¥ t^{-1})	Revenue (¥)	Update Date	Data Sources
1	Cathode material	$LiFePO_4$	95	0.2375	37510	8908.625	Dce. 27th 2024	SMM
3	Anode	Graphite	96	0.125	20400	2550	Dce. 27th 2024	SMM
4	Current collector	Al foil	90	0.0540	35200	1900.8	Dce. 27th 2024	SMM
5	Current collector	Cu foil	90	0.090	92420	8317.8	Dce. 27th 2024	Mysteel
Subtotal (¥) ***21677.23***								
Note: a) It is assumed that the level of deficiency in the spent LFP battery remains consistent ($Li_{0.8}FePO_4$) based on hydro- recovery and DSR methods. b) The proportion of each component is 25% of cathode material, 13% of graphite, 6% of Al foil, 10% of Cu foil, 3% of separator, 16% of electrolyte, and 20% of shell. c) The value of separator, electrolyte, and shell is hard to assess in the real process, therefore, these components are excluded from the revenue analysis. d) Mysteel (https://www.mysteel.com/).								

Supplementary Table 16 DSR revenue analysis.

Revenue analysis based direct separation and regeneration strategy								
No.	Item	Material	Recovery yield (%)	Production (t)	Market price (¥ t^{-1})	Revenue (¥)	Update Date	Data Sources
1	Cathode material	$LiFePO_4$	95	0.2375	37510	8908.625	Dce. 27th 2024	SMM
2	Anode	Graphite	98	0.1274	20400	2598.96	Dce. 27th 2024	SMM
3	Current collector	Al foil	90	0.0540	35200	1900.8	Dce. 27th 2024	SMM
4	Current collector	Cu foil	90	0.090	92420	8317.8	Dce. 27th 2024	Mysteel
Subtotal (¥) ***21726.19***								
Note: a) It is assumed that the level of deficiency in the spent LFP battery remains consistent ($Li_{0.8}FePO4$) based on hydro- recovery and DSR methods. b) The proportion of each component is 25% of cathode material, 13% of graphite, 6% of Al foil, 10% of Cu foil, 3% of separator, 16% of electrolyte, and 20% of shell. c) The value of separator, electrolyte, and shell is hard to assess in the real process, therefore, these components are excluded from the revenue analysis. d) Mysteel (https://www.mysteel.com/).								

Supplementary Table 17 Profit calculation.

Recovery profit results				
No.	Recycling route	Cost (¥)	Revenue (¥)	Profit (¥)
1	Hydro-	***14421.81***	***18537.64***	***4115.83***
2	DSR	***12331.87***	***21726.19***	***9583.92***
3	Hydro- synthesis	***16507.65***	***21677.23***	***5169.575***
Note: 1$ = 7.2985 ¥ (Update time: 2024/12/27).				

References

1. Y. Cao, J. Li, D. Tang, F. Zhou, M. Yuan, Y. Zhu, C. Feng, R. Shi, X. Wei, B. Wang, Y. Song, H. M. Cheng and G. Zhou, *Adv Mater*, 2024, **36**, e2414048.
2. C. Feng, Y. Cao, L. Song, B. Zhao, Q. Yang, Y. Zhang, X. Wei, G. Zhou and Y. Song, *Angew Chem Int Ed Engl*, 2024, DOI: 10.1002/anie.202418198, e202418198.
3. J. Li, R. Shi, J. Wang, Y. Cao, H. Ji, J. Tang, G. Ji, W. Chen, M. Zhang, X. Xiao and G. Zhou, *Adv Mater*, 2024, DOI: 10.1002/adma.202414235, e2414235.
4. M. Xu, C. Wu, F. Zhang, Y. Zhang, J. Ren, C. Zhang, X. Wang, L. Xiao, O. Fontaine and J. Qian, *Energy Storage Materials*, 2024, **71**, 103611.
5. X. X. Zhao, X. T. Wang, J. Z. Guo, Z. Y. Gu, J. M. Cao, J. L. Yang, F. Q. Lu, J. P. Zhang and X. L. Wu, *Advanced Materials*, 2024, DOI: 10.1002/adma.202308927.
6. Y. Xu, X. Qiu, B. Zhang, A. Di, W. Deng, G. Zou, H. Hou and X. Ji, *Green Chemistry*, 2022, **24**, 7448-7457.
7. X. Qiu, C. Wang, Y. Liu, Q. Han, L. Xie, L. Zhu and X. Cao, *Journal of Energy Storage*, 2025, **105**, 114721.
8. D. Tang, G. Ji, J. Wang, Z. Liang, W. Chen, H. Ji, J. Ma, S. Liu, Z. Zhuang and G. Zhou, *Advanced Materials*, 2023, **36**.
9. G. Ji, J. Wang, Z. Liang, K. Jia, J. Ma, Z. Zhuang, G. Zhou and H.-M. Cheng, *Nature Communications*, 2023, **14**, 584.
10. K. Jia, J. Ma, J. Wang, Z. Liang, G. Ji, Z. Piao, R. Gao, Y. Zhu, Z. Zhuang, G. Zhou and H. M. Cheng, *Advanced Materials*, 2022, **35**.
11. C. Wang, X. Qiu, G. Shen, X. Chen, J. Wang, L. Xie, Q. Han, L. Zhu, J. Li and X. Cao, *Green Chemistry*, 2024, **26**, 1501-1510.
12. Y. Xu, B. Zhang, Z. Ge, H. Wang, N. Hong, X. Xiao, B. Song, Y. Zhang, Y. Tian, W. Deng, G. Zou, H. Hou and X. Ji, *Chemical Engineering Journal*, 2023, **477**, 147201.